AIAA 2002–1483

High-Fidelity Aero-Structural Design Optimization of a Supersonic Business Jet

Joaquim R. R. A. Martins, Juan J. Alonso
Stanford University, Stanford, CA 94305

James J. Reuther
NASA Ames Research Center, Moffett Field, CA 95035

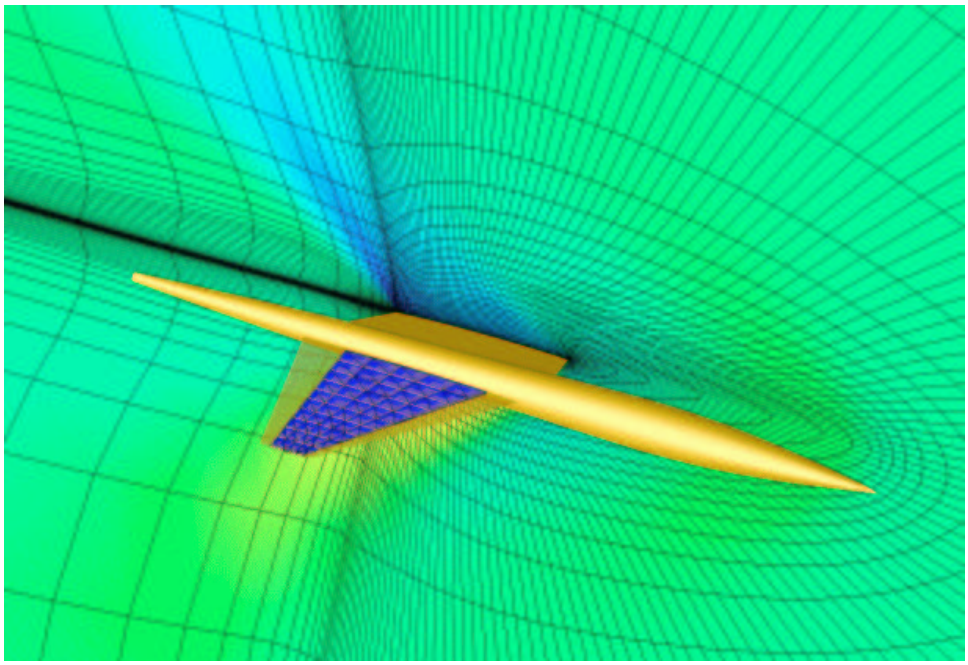

43rd AIAA/ASME/ASCE/AHS/ASC Structures, Structural Dynamics, and Materials Conference
April 22–25, 2002/Denver, CO

AIAA 2002–1483

High-Fidelity Aero-Structural Design Optimization of a Supersonic Business Jet

Joaquim R. R. A. Martins*, Juan J. Alonso†
Stanford University, Stanford, CA 94305

James J. Reuther‡
NASA Ames Research Center, Moffett Field, CA 95035

This paper focuses on the demonstration of an integrated aero-structural method for the design of aerospace vehicles. Both aerodynamics and structures are represented using high-fidelity models such as the Euler equations for the aerodynamics and a detailed finite element model for the primary structure. The aerodynamic outer mold line (OML) and a structure of fixed topology are parameterized using a large number of design variables. The aero-structural sensitivities of aerodynamic and structural cost functions with respect to both aerodynamic shape and structural variables are computed using an accurate and efficient coupled-adjoint procedure. K-S functions are used to reduce the number of structural constraints in the problem. Sample optimization results of the aerodynamic shape and structure of a natural laminar flow supersonic business jet are presented together with an assessment of the accuracy of the sensitivity information obtained using this procedure.

Introduction

A considerable amount of research has been conducted on Multi-Disciplinary Optimization (MDO) and its application to aircraft design. The survey paper by Sobieski[20] provides a comprehensive discussion of much of the work in this area. The efforts described therein range from the development of techniques for inter-disciplinary coupling to applications in real-world design problems. In most cases, sound coupling and optimization methods were shown to be extremely important since some techniques, such as sequential discipline optimization, were unable to converge to the true optimum of a coupled system. Wakayama,[21] for example, showed that in order to obtain realistic wing planform shapes with aircraft design optimization, it is necessary to include multiple disciplines in conjunction with a complete set of real-world constraints.

Aero-structural analysis has traditionally been carried out in a cut-and-try basis. Aircraft designers have a pre-conceived idea of the shape of an "optimal" load distribution and then tailor the jig shape of the structure so that the deflected wing shape under a 1-g load gives the desired distribution. While this approach is typically sufficient for traditional swept-back wing designs, the complexity of aero-structural interactions can be such that, in more advanced designs where little experience has been accumulated or where multiple design points are part of the mission, it can result in sub-optimal designs. This is the case in the design of both small and large supersonic transports, where simple beam theory models of the wing cannot be used to accurately describe the behavior of the wing structure. In some cases, these aircraft must even cruise for significant portions of their flight at different Mach numbers. In addition, a variety of studies show that supersonic transports exhibit a range of undesirable aeroelastic phenomena due to the low bending and torsional stiffness that result from wings with low thickness to chord ratio. These phenomena can only be suppressed when aero-structural interactions are taken into account at the preliminary design stage.[3]

Unfortunately, the modeling of the participating disciplines in most of the work that has appeared so far has remained at a relatively low level. While useful at the conceptual design stage, lower-order models cannot accurately represent a variety of nonlinear phenomena such as wave drag, which can play an important role in the search for the optimum design. An exception to this low-fidelity modeling is the recent work by Giunta[6] and by Maute et al.[14] where aero-structural sensitivities are calculated using higher-fidelity models.

The ultimate objective of our work is to develop an MDO framework for high-fidelity analysis and optimization of aircraft configurations. The framework is built upon prior work by the authors on aero-structural high-fidelity sensitivity analysis.[11,17] The objective of this paper is to present the current ca-

*Doctoral Candidate, AIAA Member
†Assistant Professor, AIAA Member
‡Research Scientist, AIAA Associate Fellow

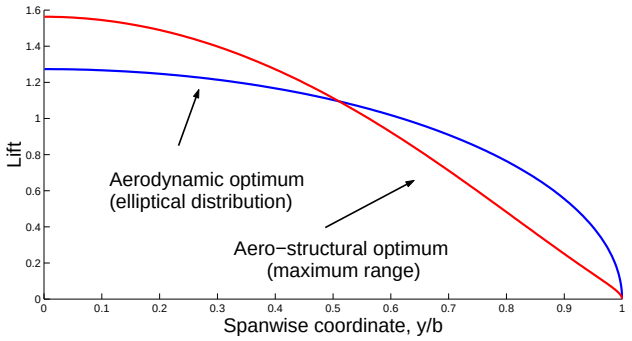

Fig. 1 Elliptic vs. aero-structural optimum lift distribution.

pability of this framework and to demonstrate it by performing a simplified aero-structural design of a supersonic business jet configuration.

The following sections begin with the description of the aircraft optimization problem we propose to solve. We then introduce the adjoint method for the calculation of sensitivities and derive the sensitivity equations for the aero-structural system. A detailed study of the accuracy of the aeroelastic sensitivity information is also presented for validation purposes. Finally we present results of the application of our sensitivity analysis method to two supersonic business jet design cases.

Aircraft Optimization Problem

For maximum lift-to-drag ratio, it is a well know result from classical inviscid aerodynamics that a wing must exhibit an elliptic lift distribution. For aircraft design, however, it is usually not the lift-to-drag ratio we want to maximize but an objective function that reflects the overall mission of the particular aircraft. Consider, for example, the Breguet range formula

$$R = \frac{V}{c}\frac{C_L}{C_D}\ln\frac{W_i}{W_f}, \tag{1}$$

where V is the cruise velocity and c is the specific fuel consumption of the powerplant. C_L/C_D is the ratio of lift to drag, and W_i/W_f is the ratio of initial and final cruise weights of the aircraft.

The Breguet range equation expresses a trade-off between the drag and the empty weight of the aircraft and constitutes a reasonable objective function to use in aircraft design. If we were to parameterize a design with both aerodynamic and structural variables and then maximized the range for a fixed initial cruise weight, subject to stress constraints, we would obtain a lift distribution similar to the one shown in Figure 1.

This optimum lift distribution trades off the drag penalty associated with unloading the tip of the wing, where the loading contributes most to the maximum stress at the root of the wing structure, in order to reduce the weight. The end result is an increase in

Fig. 2 Natural laminar flow supersonic business jet configuration.

range when compared to the elliptically loaded wing that results from an increased weight fraction W_i/W_f. The result shown in Figure 1 illustrates the need for taking into account the coupling of aerodynamics and structures when performing aircraft design.

The aircraft configuration that is the focus of this work is that of the supersonic business jet shown in Figure 2. This configuration is being developed by the ASSET Research Corporation and it is designed to achieve a large percentage of laminar flow on the low-sweep wing, resulting in decreased friction drag.[9] The aircraft is to fly at Mach 1.5 and have a range of 5,300 nautical miles.

Detailed mission analysis for this aircraft has determined that one count of drag ($\Delta C_D = 0.0001$) is worth 310 pounds of empty weight. This means that to optimize the configuration we can minimize the objective function

$$I = \alpha C_D + \beta W, \tag{2}$$

where C_D is the drag coefficient, W is the structural weight in pounds and $\alpha/\beta = 3.1 \times 10^6$.

We will parameterize the design using an arbitrary number of shape design variables that modify the Outer Mold Line (OML) of the aircraft (x_A) and structural design variables that dictate the thicknesses of the structural elements (x_S). In this work, the topology of the structure remains unchanged, i.e. the number of spars and ribs and their planform-view location is fixed. However, the depth and thickness of the structural members is still allowed to change with variations of the OML.

Among the constraints to be imposed, the most obvious one is that during cruise the lift must equal the weight of the aircraft. In our optimization problem we constrain the C_L by periodically adjusting the angle-of-attack within the aero-structural solution and assume that the aircraft will adjust its altitude to obtain the desired lift.

We also must constrain the stresses so that the yield stress of the material is not exceeded at a number

of load conditions. There are typically thousands of finite-elements describing the structure of the aircraft, and it can become computationally very costly to treat these constraints separately. The reason for this high cost is that although there are efficient ways of computing sensitivities of a few functions with respect to many design variables, and for computing sensitivities of many functions with respect to a few design variables, there is no known efficient method for computing sensitivities of many functions with respect to many design variables.

For this reason, we lump the individual element stresses using Kreisselmeier-Steinhauser (K-S) functions. In the limit, all element stress constraints can be lumped into a single K-S function, thus minimizing the cost of a large-scale aero-structural design cycle. Suppose that we have the following constraint for each structural finite element,

$$g_i = 1 - \frac{\sigma_{i_{VM}}}{\sigma_{yield}} \geq 0, \tag{3}$$

where $\sigma_{i_{VM}}$ is the element von Mises stress and σ_{yield} is the yield stress of the material. The corresponding K-S function is defined as

$$\mathrm{KS}\left(g_i(x)\right) = -\frac{1}{\rho} \ln \left[\sum_i \mathrm{e}^{-\rho g_i(x)} \right]. \tag{4}$$

This function represents a lower bound envelope of all the constraint inequalities and ρ is a positive parameter that expresses how close this bound is to the actual minimum of the constraints. This constraint lumping method is conservative and may not achieve the exact same optimum that a problem treating the constraints separately would. However, the use of K-S functions has been demonstrated and it constitutes a viable alternative, being effective in optimization problems with thousands of constraints.[2]

Having defined our objective function, design variables and constraints, we can now summarize the aircraft design optimization problem as follows:

$$\begin{aligned} \text{minimize} \quad & I = \alpha C_D + \beta W \\ x_A, x_S \in \mathbb{R}^n & \\ \text{subject to} \quad & C_L = C_{L_T} \\ & \mathrm{KS} \geq 0 \\ & x_S \geq x_{S_{\min}}. \end{aligned}$$

The stress constraints in the form of K-S functions must be enforced by the optimizer for aerodynamic loads corresponding to a number of flight conditions. Finally, a minimum gage is specified for each structural element thickness.

Analytic Sensitivity Analysis

When solving an optimization problem the goal is typically to minimize an *objective function*, I, by carefully choosing the values of a set of *design variables* and satisfying the constraints of the problem. In general, the objective function depends not only on the design variables, but also on the physical state of the problem that is being modeled. Thus we can write

$$I = I(x_j, y_k), \tag{5}$$

where x_j represents the design variables and y_k is the symbol for the state variables.

For a given vector x_j, the solution of the governing equations of the system yields a vector y_k, thus establishing the dependence of the state of the system on the design variables. We will denote the governing equations as

$$R_{k'}\left(x_j, y_k\left(x_j\right)\right) = 0. \tag{6}$$

The first instance of x_j in the above equation signals the fact that the residual of the governing equations may depend *explicitly* on x_j. In the case of a structural solver, for example, changing the size of an element has a direct effect on the stiffness matrix. By solving the governing equations we determine the state, y_k, which depends *implicitly* on the design variables through the solution of the system.

Since the number of equations must equal the number of state variables, the ranges of the indices k and k' are the same, i.e., $k, k' = 1, \ldots, n_R$. For a structural solver, for example, n_R is the number of degrees of freedom, while for a Computational Fluid Dynamics (CFD) solver, n_R is the number of mesh points multiplied by the number of state variables at each point (four in the two-dimensional case and five in three dimensions.) For a coupled system, R'_k represents *all* the governing equations of the different disciplines, including their coupling.

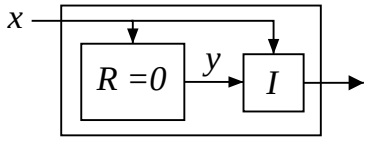

Fig. 3 Schematic representation of the governing equations ($R = 0$), design variables (x), state variables (y), and objective function (I), for an arbitrary system.

A graphical representation of the system of governing equations is shown in Figure 3, with the design variables x_j as the inputs and I as the output. The two arrows leading to I illustrate the fact that the objective function typically depends on the state variables and may also be an explicit function of the design variables.

When solving the optimization problem using a gradient-based optimizer, the *total* variation of the objective function with respect to the design variables, $\frac{\mathrm{d}I}{\mathrm{d}x_j}$, must be calculated. As a first step towards obtaining this total variation, we use the chain rule to

write the total variation of I as

$$\delta I = \frac{\partial I}{\partial x_j}\delta x_j + \frac{\partial I}{\partial y_k}\delta y_k, \tag{7}$$

for $k = 1, \ldots, n_R$, $j = 1, \ldots, n_x$, where we use indicial notation to denote the vector dot products. If we were to use this equation directly, the vector of δy_k's would have to be calculated for each δx_j by solving the governing equations n_x times. If there are many design variables and the solution of the governing equations is costly (as is the case for large coupled iterative analyses), using equation (7) directly can be impractical.

We now observe that the variations δx_j and δy_k in the total variation of the objective function (7) are not independent of each other since the perturbed system must always satisfy equation (6). A relationship between these two sets of variations can be obtained by realizing that the variation of the residuals (6) must be zero, i.e.

$$\delta R_{k'} = \frac{\partial R_{k'}}{\partial x_j}\delta x_j + \frac{\partial R_{k'}}{\partial y_k}\delta y_k = 0, \tag{8}$$

for all $k = 1, \ldots, n_R$ and $j = 1, \ldots, n_x$.

Since this residual variation (8) is zero we can add it to the objective function variation (7) without modifying the latter, i.e.

$$\delta I = \frac{\partial I}{\partial x_j}\delta x_j + \frac{\partial I}{\partial y_k}\delta y_k + \psi_{k'}\left(\frac{\partial R_{k'}}{\partial x_j}\delta x_j + \frac{\partial R_{k'}}{\partial y_k}\delta y_k\right), \tag{9}$$

where $\psi_{k'}$ are arbitrary scalars we will call *adjoint variables*. This approach is identical to the one used in non-linear constrained optimization, where equality constraints are added to the objective function, and the arbitrary scalars are known as *Lagrange multipliers*. The problem then becomes an unconstrained optimization problem, which is more easily solved.

We can now group the terms in equation (9) that contribute to the same variation and write

$$\delta I = \left(\frac{\partial I}{\partial x_j} + \psi_{k'}\frac{\partial R_{k'}}{\partial x_j}\right)\delta x_j + \left(\frac{\partial I}{\partial y_k} + \psi_{k'}\frac{\partial R_{k'}}{\partial y_k}\right)\delta y_k. \tag{10}$$

If we set the term multiplying δy_k to zero, we are left with the total variation of I as a function of the design variables and the adjoint variables, removing the dependence of the variation on the state variables. Since the adjoint variables are arbitrary, we can accomplish this by solving the *adjoint equations*

$$\frac{\partial R_{k'}}{\partial y_k}\psi_{k'} = -\frac{\partial I}{\partial y_k}. \tag{11}$$

These equations depend only on the partial derivatives of both the objective function and the residuals of the governing equations with respect to the state variables. Since these partial derivatives can be calculated directly without solving the governing equations, the adjoint equations (11) only need to be solved once for each I and their solution is valid for all the design variables.

When adjoint variables are found in this manner, we can use them to calculate the total sensitivity of I with the first term of equation (10), i.e.

$$\frac{\mathrm{d}I}{\mathrm{d}x_j} = \frac{\partial I}{\partial x_j} + \psi_{k'}\frac{\partial R_{k'}}{\partial x_j}. \tag{12}$$

The cost involved in calculating sensitivities using the adjoint method is practically independent of the number of design variables. After having solved the governing equations, the adjoint equations are solved only once for each I. The terms in the adjoint equations are inexpensive to calculate, and the cost of solving the adjoint equations is similar to that involved in the solution of the governing equations.

The adjoint method has been widely used for single discipline sensitivity analysis and examples of its application include structural sensitivity analysis[1] and aerodynamic shape optimization.[8,15,16]

Aero-Structural Sensitivity Analysis

We will now use the equations derived in the previous section to write down the adjoint sensitivity equations specific to the aero-structural system. In this case we have coupled aerodynamic (R_A) and structural (R_S) governing equations, and two sets of state variables: the flow state vector, w, and the vector of structural displacements, u. In the following expressions, we no longer use index notation and we split the vectors of residuals, states and adjoints into two smaller vectors corresponding to the aerodynamic and structural systems, i.e.

$$R_{k'} = \begin{bmatrix} R_A \\ R_S \end{bmatrix}, \quad y_k = \begin{bmatrix} w \\ u \end{bmatrix}, \quad \psi_{k'} = \begin{bmatrix} \psi_A \\ \psi_S \end{bmatrix}. \tag{13}$$

Figure 4 shows a diagram representing the coupling in this system.

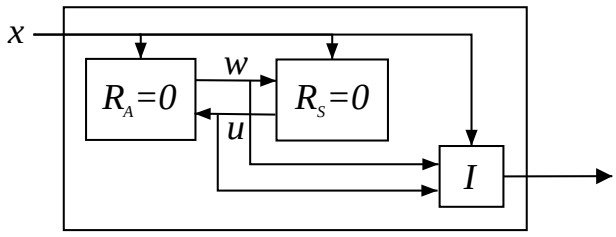

Fig. 4 Schematic representation of the aero-structural governing equations.

Using this new notation, the adjoint equation (11) for an aero-structural system can be written as

$$\begin{bmatrix} \frac{\partial R_A}{\partial w} & \frac{\partial R_A}{\partial u} \\ \frac{\partial R_S}{\partial w} & \frac{\partial R_S}{\partial u} \end{bmatrix}^T \begin{bmatrix} \psi_A \\ \psi_S \end{bmatrix} = - \begin{bmatrix} \frac{\partial I}{\partial w} \\ \frac{\partial I}{\partial u} \end{bmatrix}. \qquad (14)$$

In addition to the diagonal terms of the matrix that appear when we solve the single discipline adjoint equations, we also have off-diagonal terms expressing the sensitivity of one discipline to the state variables of the other. The residual sensitivity matrix in this equation is identical to that of the Global Sensitivity Equations (GSE) introduced by Sobieski.[19] Considerable detail is hidden in the terms of this matrix and we will describe each one of them for clarity.

- $\partial R_A/\partial w$: This term represents the variation of the residuals of the CFD equations due to changes in the the flow variables. When a flow variable at a given cell center is perturbed, the sum of the fluxes on that cell is altered. Only that cell and its neighbors are affected. Therefore, even though $\partial R_A/\partial w$ is a large square matrix, it is also extremely sparse and its non-zero terms can be easily calculated. In our solvers this matrix is not stored explicitly.

- $\partial R_A/\partial u$: This derivative represents the effect that the structural displacements have on the residuals of the CFD solution through the perturbation of the CFD mesh. When the wing deflects, the mesh must be warped, resulting in a change in the geometry of a subset of grid cells. Even though the flow variables are kept constant, the change in the geometry has an influence on the sum of the fluxes, whose variation can be easily obtained by re-calculating the residuals for the warped cells.

- $\partial R_S/\partial w$: The linear structural equations can be written as $R_S = Ku - f = 0$, where K is the stiffness matrix and f is the vector of applied forces. The only term that the flow variables affect directly is the applied force, and therefore this term is equal to $-\partial f/\partial w$, which can be found by examining the procedure that integrates the pressures in the CFD mesh and transfers them to the structural nodes to obtain the applied forces.

- $\partial R_S/\partial u$: Since the forces do not depend directly on the displacements and neither does K (for a linear model), this term is simply the stiffness matrix, K.

The right-hand side terms depend on the function of interest, I. In our case, we have two different functions we are interested in: the coefficient of drag, C_D, and the K-S function. When $I = C_D$ we have,

- $\partial C_D/\partial w$: The direct sensitivity of the drag coefficient to the flow variables can be obtained analytically by examining the numerical integration of the surface pressures that produce C_D.

- $\partial C_D/\partial u$: This term represents the change in the drag coefficient due to the displacement of the wing while keeping the pressure distribution constant. The structural displacements affect the drag directly, since they change the wing surface geometry over which the pressure distribution is integrated.

When $I = \mathrm{KS}$,

- $\partial \mathrm{KS}/\partial w$: This term is zero, since the stresses do not depend explicitly on the loads.

- $\partial \mathrm{KS}/\partial u$: The stresses depend directly on the displacements since $\sigma = Su$. This term is therefore equal to $[\partial \mathrm{KS}/\partial \sigma]\, S$.

Since the factorization of the full matrix in the system of equations (14) would be extremely costly, our approach uses an iterative solver, much like the one used for the aero-structural solution, where the adjoint vectors are *lagged* and the two different sets of equations are solved separately. For the calculation of the adjoint vector of one discipline, we use the adjoint vector of the other discipline from the previous iteration, i.e., we solve

$$\left[\frac{\partial R_A}{\partial w}\right]^T \psi_A = -\frac{\partial I}{\partial w} - \left[\frac{\partial R_S}{\partial w}\right]^T \tilde{\psi}_S, \qquad (15)$$

$$\left[\frac{\partial R_S}{\partial u}\right]^T \psi_S = -\frac{\partial I}{\partial u} - \left[\frac{\partial R_A}{\partial u}\right]^T \tilde{\psi}_A, \qquad (16)$$

where $\tilde{\psi}_A$ and $\tilde{\psi}_S$ are the lagged aerodynamic and structural adjoint vectors. The final result given by this system, is the same as that of the original coupled-adjoint equations (14). We will call this the *Lagged-Coupled Adjoint* (LCA) method for computing sensitivities of coupled systems. Note that these equations look like the single discipline adjoint equations for the aerodynamic and the structural solvers, with the addition of forcing terms in the right-hand-side that contain the off-diagonal terms of the residual sensitivity matrix. Note also that, even for more than two disciplines, this iterative solution procedure is nothing but the well-known Block-Jacobi method.

As noted previously, $\partial R_S/\partial u = K$ for a linear structural solver. Since the stiffness matrix is symmetric ($K^T = K$) the structural equations (16) are self-adjoint. Therefore, the structural solver can be used to solve for the structural adjoint vector, ψ_S, by using the *pseudo-load* vector given by the right-hand-side of equation (16).

Once both adjoint vectors have converged, we can compute the final sensitivities of the objective function by using

$$\frac{\mathrm{d}I}{\mathrm{d}x} = \frac{\partial I}{\partial x} + \psi_A^T \frac{\partial R_A}{\partial x} + \psi_S^T \frac{\partial R_S}{\partial x}, \qquad (17)$$

which is the coupled version of the total sensitivity equation (12). We will now describe the last two partial derivatives in the above equation.

- $\partial R_A/\partial x$: The direct effect of aerodynamic shape perturbations on the CFD residuals is similar to that of the displacements on the same residuals, $\partial R_A/\partial u$, that we mentioned previously. The structural thicknesses of the structural finite elements do not affect the CFD residuals.

- $\partial R_S/\partial x$: The design variables have a direct effect on both the stiffness matrix and the load. Although this partial derivative is taken for a constant surface pressure field, a variation in the OML will affect the translation of these pressures to structural loads. Hence this partial derivative is equal to $\partial K/\partial x \cdot u - \partial f/\partial x$.

For the $\partial I/\partial x$ term we have again two different cases: $I = C_D$ and $I = \mathrm{KS}$. For each of these cases:

- $\partial C_D/\partial x$: This is the change in the drag coefficient due to wing-shape perturbations, while keeping the pressure distribution constant. This sensitivity is analogous to the partial derivative $\partial C_D/\partial u$ that we described above and can be easily calculated using finite-differences. For structural variables that do not affect the OML, this term is zero.

- $\partial \mathrm{KS}/\partial x$: This term represents the variation of the lumped stresses for fixed loads and displacements. When the OML is perturbed, the stresses in a given element can vary under these conditions if its shape is distorted.

As in the case of the partial derivatives in equations (14), all the terms can be computed without incurring a large computational cost since none of them involve the solution of the governing equations.

In order to solve the aircraft optimization problem we proposed earlier on, we also need sensitivities of the structural weight with respect to the design variables. Since the aero-structural coupling does not involve the weight, these sensitivities are easily computed.

Results

In this section we present the results of the application of our sensitivity calculation method to the problem of aero-structural design of a supersonic, natural laminar flow, business jet. Before describing the results of our design experience, we present the aero-structural analysis framework and the results of a sensitivity validation study.

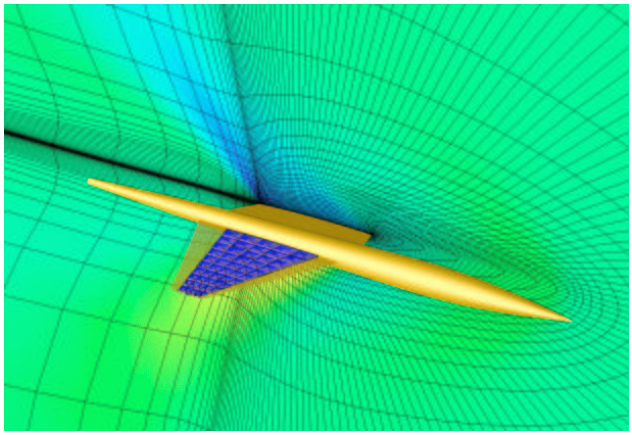

Fig. 5 Aero-structural model and solution of the supersonic business jet configuration, showing a slice of the grid and the internal structure of the wing.

Aero-Structural Analysis

The coupled-adjoint procedure was implemented as a module that was added to the aero-structural design framework previously developed by the authors.[11,17] The framework consists of an aerodynamic analysis and design module (which includes a geometry engine and a mesh perturbation algorithm), a linear finite-element structural solver, an aero-structural coupling procedure, and various pre-processing tools that are used to setup aero-structural design problems. The multi-disciplinary nature of this solver is illustrated in Figure 5 where we can see the aircraft geometry, the flow mesh and solution, and the primary structure inside the wing.

The aerodynamic analysis and design module, SYN107-MB,[16] is a multiblock parallel flow solver for both the Euler and the Reynolds Averaged Navier-Stokes equations that has been shown to be accurate and efficient for the computation of the flow around full aircraft configurations.[18] An aerodynamic adjoint solver is also included in this package in order to perform aerodynamic shape optimization in the absence of aero-structural interaction.

The structural analysis package is FESMEH, a finite element solver developed by Holden.[7] The package is a linear finite-element solver that incorporates two element types and computes the structural displacements and stresses of wing structures. Although this solver is not as general as some commercially-available packages, it is still representative of the challenges involved in using large models with tens of thousands of degrees of freedom. High-fidelity coupling between the aerodynamic and the structural analysis programs is achieved using a linearly consistent and conservative scheme.[4,17]

The structural model of the wing can be seen in Figure 5 and is constructed using a wing box with six spars evenly distributed from 15% to 80% of the chord.

Ribs are distributed along the span at every tenth of the semispan. A total of 640 finite elements were used in the construction of this model. Appropriate thicknesses of the spar caps, shear webs, and skins were chosen according to the expected loads for this design.

Aero-Structural Sensitivity Validation

In order to gain confidence in the effectiveness of the coupled aero-structural adjoint sensitivities for use in design optimization, we must ensure that the values of the gradients are accurate. For this purpose, we have chosen to validate the four sets of sensitivities discussed below. The exact value of these sensitivities is calculated using the complex-step derivative approximation.

The complex-step is a relatively new method that computes the sensitivities dI/dx_j using the formula

$$\frac{\mathrm{d}I}{\mathrm{d}x_j} \approx \frac{\mathrm{Im}\left[I\left(x_j + ih\right)\right]}{h}, \quad i = \sqrt{-1} \tag{18}$$

with second order accuracy. Details of this simple yet powerful approximation can be found in earlier work published by the authors.[10,12,13] As in the case of finite-differences, the cost of a full gradient calculation scales linearly with the total number of design variables and therefore we do not use this method in actual design. Unlike finite-differences, however, the accuracy of the complex-step method is extremely insensitive to the step size, h, making it much more robust.

In this sensitivity study two different functions were considered: the drag coefficient, C_D, and the K-S function of the stresses. Sensitivities of these two quantities with respect to both OML and structural variables are computed. The OML design variables are shape perturbations in the form of Hicks-Henne *bump* functions,[16] which not only control the aerodynamic shape of the aircraft configuration, but also change the internal structure. For example, if a perturbation increases the thickness of the wing at a specific location, the height of the spars at that point will also increase. The second set of design variables — the structural variables — are the thicknesses of the triangular plate elements that model the skin and spars of the wing.

The values of the aero-structural sensitivities of drag coefficient with respect to shape perturbations are shown in Figure 6. The ten shape perturbations were chosen to be Hicks-Henne bumps distributed chordwise on the upper surface of two adjacent airfoils around the quarter span. The plot shows very good agreement between the coupled-adjoint and the complex-step results, the average relative error between the two being 3.5%.

Figure 7 also shows the sensitivity of the drag coefficient, this time with respect to the thicknesses of five skin groups and five spar groups distributed along the span. This time the agreement is even better; the average relative error is only 1.6%.

The sensitivities of the K-S function with respect to the two sets of design variables described above are shown in Figures 8 and 9. The results show that the coupled-adjoint sensitivities are extremely accurate, with average relative errors of 2.9% and 1.6%. In Figure 9 we observe that the sensitivity of the K-S function with respect to the first structural thickness is much higher than the remaining sensitivities. This is because that particular structural design variable corresponds to the thickness of the top and bottom skins of the wing bay closest to the root, where the stress is the highest for this design case.

Note that all these sensitivities are *total* sensitivities in the sense that they account for the coupling between aerodynamics and structures. For example, a perturbation of the shape of the wing results in changes in the surface pressures and geometry that directly affect the drag. Those changes in surface pressure create a different displacement field which itself has an effect on the flow field. This coupling is fully accounted for in the coupled-adjoint method.

The cost of the sensitivity calculation using either the finite-difference or complex-step methods is linearly dependent on the number of design variables in the problem, whereas the cost of the coupled-adjoint procedure is essentially independent of this number. In more realistic design situations where the number of design variables chosen to parameterize the surface is much larger than 20, the computational efficiency of the adjoint sensitivity calculation would become even more obvious.

The cost of a finite-difference gradient evaluation for the 20 design variables is about 15 times the cost of a single aero-structural solution for computations that have converged 5.5 orders of magnitude. Notice that one would expect this method to incur a computational cost equivalent to 21 aero-structural solutions (the solution of the baseline configuration plus one flow solution for each design variable perturbation.) The cost is lower than this because the additional calculations do not start from a uniform flow-field initial condition, but from the previously converged solution.

The cost of the complex-step method is more than twice of that of the finite-difference procedure since the function evaluations require complex arithmetic. We feel, however, that the complex-step calculations are worth this cost penalty since there is no need to find an acceptable step size a priori, as in the case of the finite-difference approximations.

Finally, the coupled-adjoint method requires the equivalent of 7.5 aero-structural solutions to compute the coupled gradient. As mentioned previously, this computational cost is practically independent of the total number of design variables in the problem and would therefore remain at a similar value, even in the more realistic case of 200 or more design variables. In

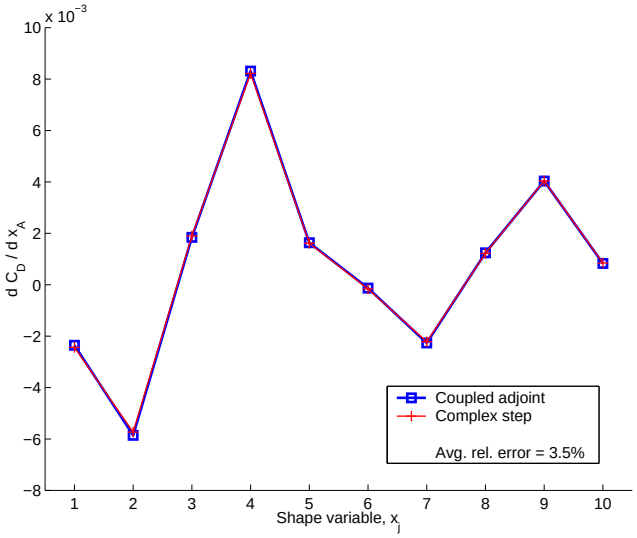

Fig. 6 Sensitivities of the drag coefficient with respect to shape perturbations.

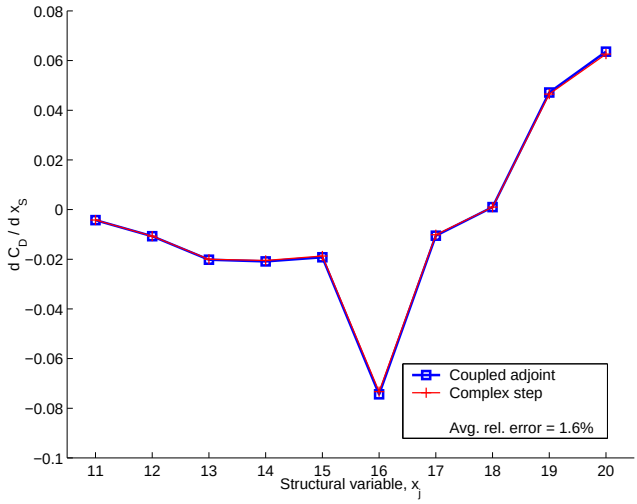

Fig. 7 Sensitivities of the drag coefficient with respect to structural thicknesses.

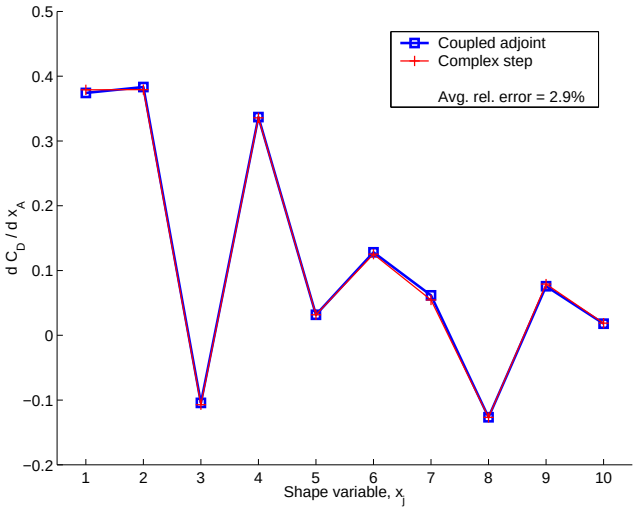

Fig. 8 Sensitivities of the K-S function with respect to shape perturbations.

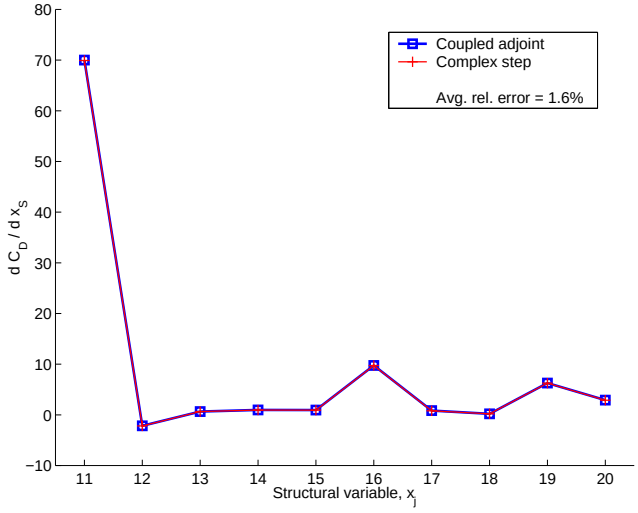

Fig. 9 Sensitivities of the K-S function with respect to structural thicknesses.

contrast, the finite-difference method would require a computational effort of around $\frac{200}{20} \times 15 = 150$ times the cost of an aero-structural solution to compute the same gradient, which is impractical within industrial design environments, even with current state-of-the-art parallel computing systems.

Aerodynamic Design

In order to establish an upper limit for the potential improvements that can be realized with the use of the aero-structural design framework, we first carried out an aerodynamic shape optimization that assumes a rigid configuration. For the natural laminar flow supersonic business jet, the total inviscid drag at $C_L = 0.1$ is $C_D = 0.0074$. Of this total inviscid drag, with an aspect ratio $\mathcal{AR} = 3.0$ and a span efficiency factor of 0.95, the lift-induced drag is $C_{D_i} = 0.0011$. The remaining amount of drag ($\Delta C_D = 0.0063$) arises from the volume- and lift-dependent contributions of the wave drag. Using linear theory, the lift-dependent portion of the drag turns out to be $C_{D_{lift-dep}} = 0.0047$, and the volume-dependent part is the remaining $C_{D_{vol-dep}} = 0.0016$. Our aerodynamic optimization cannot decrease the C_{D_i} significantly, since the spanload distribution is nearly optimal. If the volume of the wing-fuselage combination remains constant, $C_{D_{vol-dep}}$ will not change. The only other option to reduce drag in an inviscid setting is to redistribute the total lift in such a way that $C_{D_{lift-dep}}$ is minimized by arriving at a lift distribution that is roughly elliptic in the streamwise direction. For these reasons, reductions in drag as small as one count are quite significant in supersonic design. In general terms, a one count reduction corresponds to approximately 1% of the total drag of the airplane.

In order to parameterize the shape of the aircraft, we

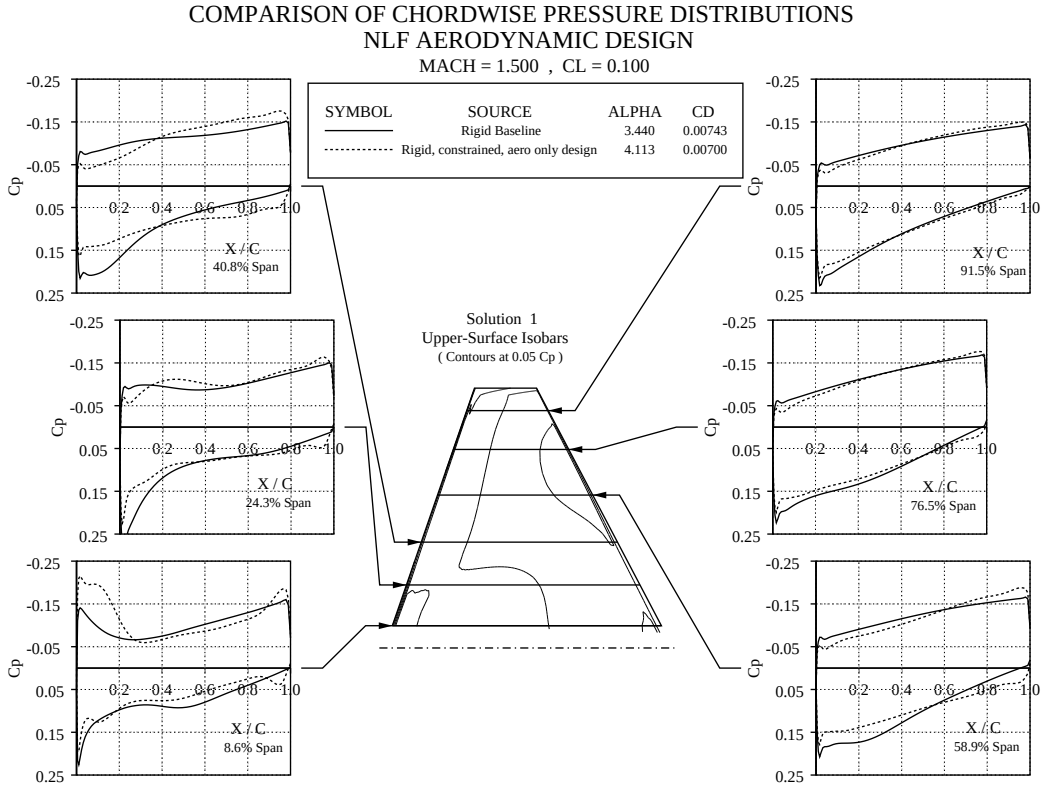

Fig. 10 Wing pressure distributions for rigid baseline and aerodynamic optimized cases.

have chosen sets of design variables that apply to both the wing and the fuselage. The wing shape is modified by the design optimization procedure at six defining stations uniformly distributed from the side-of-body to the tip of the wing. The shape modifications of these defining stations are linearly lofted to a zero value at the previous and next defining stations. On each defining station, the twist, the leading and trailing edge camber distributions, and five Hicks-Henne bump functions on both the upper and lower surfaces are allowed to vary. The leading and trailing edge camber modifications are not applied at the first defining station. This yields a total of 76 design variables on the wing. Planform modifications are not allowed in this parameterization. In order to prevent the optimizer from thinning the wing to an unreasonable degree, 5 thickness constraints are added to each of the defining stations for a total of 30 linear constraints. The shape of the fuselage is parameterized in such a way that its camber is allowed to vary, but the total volume and cross-sectional shape remain constant. This is accomplished with 9 bump functions evenly distributed in the streamwise direction starting at the 10% fuselage station. Fuselage nose and trailing edge camber functions are added to the fuselage camber distribution in a similar way to what was done with the wing sections.

The complete configuration is therefore parameterized with a total of 87 design variables and 30 linear constraints. As mentioned in an earlier section, the cost of aero-structural gradient information using our coupled-adjoint method is effectively independent of the number of design variables: in more realistic full configuration test cases that we are about to tackle, 500 or more design variables are often necessary to describe the shape variations of the configuration (including nacelles, diverters, and tail surfaces.)

The objective in this optimization is to minimize the value of C_D of the configuration at constant $C_L = 0.1$ while maintaining the thickness of the wing. All optimization work was carried out using the non-linear constrained optimizer NPSOL.[5] Euler calculations are performed on a 36-block multiblock mesh that is constructed from the decomposition of a $193 \times 33 \times 49$ C-H mesh. During the process of the optimization, all flow evaluations are converged to 5.5 orders of magnitude of the average density residual and the C_L constraint is achieved to within 10^{-6}.

Figure 10 shows a comparison of the pressure distributions of the baseline (rigid) geometry and those of the optimized design after 10 design iterations. The coefficient of drag of the complete aircraft has decreased by 5.8% from $C_{D_0} = 0.00743$ to $C_D = 0.0070$. This decrease in the drag of the configuration is partially achieved by streamwise redistribution of the lift

at all spanwise stations. The thickness distribution is maintained due to the imposition of the thickness constraints. Interestingly, the angle of attack of the optimized configuration has increased by almost 0.7° which is an indication that the original wing mounting angle, along the axis of the fuselage, was not optimal. A substantial portion of the decrease in drag is obtained from the fuselage camber modifications. In fact, from the results of two separate design calculations where the fuselage and wing were modified while keeping the shape of the other fixed, it is clear that nearly one-half of the drag decrease results from fuselage camber modifications alone. The streamwise redistribution of lift achieved with these modifications is quite effective in spreading the lift along the length of the aircraft. The final shape of the fuselage (for a different test case) can be seen in Figure 14.

The exact same optimization was also carried out while allowing the configuration to undergo aeroelastic deformations. The sensitivities of C_D with respect to the aerodynamic design variables are now computed using the coupled structural adjoint procedure. Notice that while no structural design variables are present in this test case, the depths of the ribs and spars follow the shape of the OML of the aircraft. Figure 11 shows the resulting pressure distributions after 9 design iterations. Notice that an almost identical reduction in C_D was obtained in this case. This fact is an indirect validation of the coupled-adjoint sensitivity analysis procedure since the optimization is able to recover a very similar solution to the rigid case in the presence of aeroelastic deformations. For an aircraft that operates at a single cruise point, the typical approach would be to consider the outcome of the first design case the 1-g shape and to construct a jig shape that would deflect to this geometry under cruise loads.

Aero-Structural Design

The initial application of our design methodology to the aero-structural design of a supersonic business jet is simply a proof-of-concept problem meant to validate the sensitivities obtained with our method. Current work is addressing the use of multiple, realistic load conditions, proper imposition of non-linear stress constraints, and the addition of diverters, nacelles, and empennage.

As an intermediate step before we include non-linear constraints based on load cases that result from a number of different flight conditions, we decided to restrict ourselves to the cruise condition and test the sensitivities of the lumped stress function, KS, by using the following objective function,

$$I = \alpha C_D + \beta W + \gamma \max(0, -\mathrm{KS})^2. \qquad (19)$$

In the results to be presented, the values $\alpha = 10^4$, $\beta = 3.226 \times 10^{-3}$, and $\gamma = 10^3$ are used. Note that the scalars that multiply the structural weight, W, and the

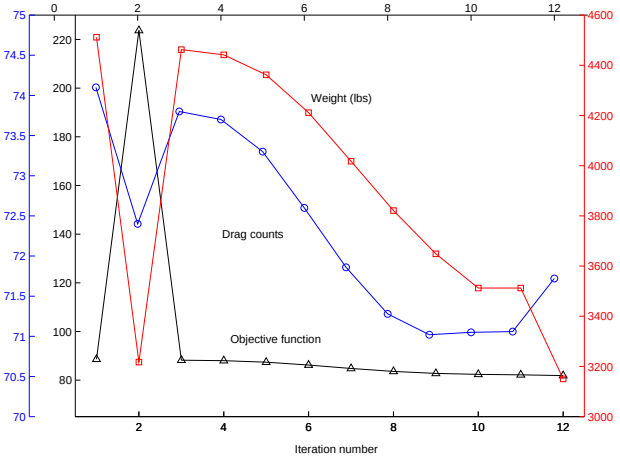

Fig. 12 Iteration history for the aero-structural optimization.

coefficient of drag, C_D, reflect the correct trade-off between drag and weight that was previously mentioned, i.e. that one count of drag is worth 310 pounds of weight. Notice also that instead of imposing the stress constraints as separate non-linear constraints (which the optimizer is able to handle), we have initially opted for adding them as a large positive penalty function to the objective of the optimization. Due to the nature of the KS function, it was necessary to zero out the contribution of this penalty when the stress constraints were not violated. This functional dependence makes the curvature of the penalty function discontinuous near the fully stressed condition and can therefore confuse the optimizer. This would not be the case had the constraints been properly imposed.

For this design case we use the same aerodynamic variables we used for the previous design cases with the addition of 20 structural design variables. The first 10 are related to the skin thicknesses of the top and bottom surfaces of the wing. Each group consists of the plate elements located between two adjacent ribs. The remaining structural variables are the thicknesses of the plate elements that model the spars of the wing. Again, each group is composed of the plates between two adjacent ribs. All structural design variables are constrained to exceed a pre-specified minimum gage value.

Notice that given the construction of the cost function, I, the incentive on the part of the optimizer is in decreasing the drag and weight of the structure in appropriate combinations. The large penalty imposed on the violation of the stress constraints effectively prevents further weight reductions by decreasing the size of the structural variables. However, optimum designs may not be those with minimum drag (if the weight can be reduced significantly at the expense of a small increase in C_D) or minimum weight (if a slightly higher weight can allow for a lower overall C_D).

Figure 12 shows the evolution of this aero-structural

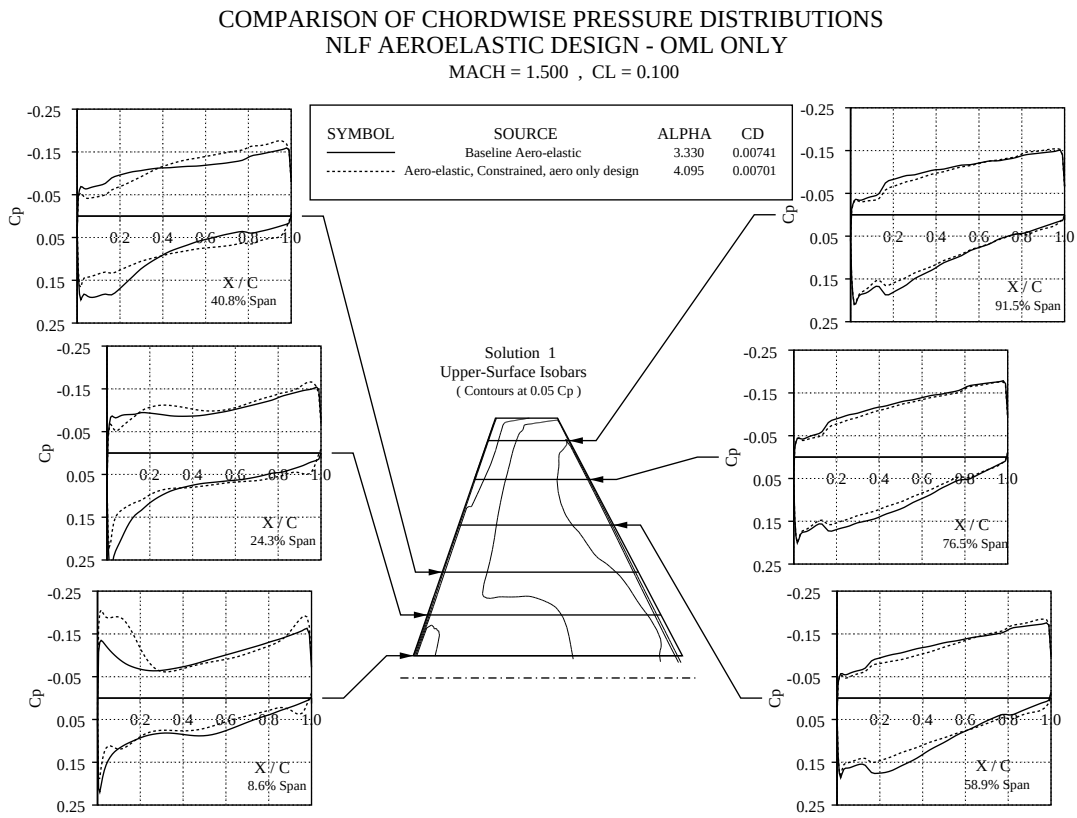

Fig. 11 Wing pressure distributions for aero-structural baseline and optimized cases, OML design variables only.

design case for successive design iterations. In the figure, we can see the values of the coefficient of drag (in counts), the wing structural weight (in lbs), and the value of the composite cost function. Notice that at iteration 2, the stress constraint is violated, resulting in a large increase in the penalty function and the overall objective function. As the iterations progress, the C_D decreases from 74.1 counts to 71.7 counts, while the weight of the structure also decreases from 4511 lbs to 3150 lbs. In the last iteration the drag goes up but this is offset by a substantial decrease in the weight of the structure in such a way that the overall objective function also decreases. Notice that the pitching moment coefficient is practically unchanged, and, therefore, no trim drag penalty needs to be taken into account.

Since the loads for this simplified case are specified at the cruise condition, the optimizer attempts to decrease the structural thicknesses to the point where the structure is nearly fully stressed. A close look at the maximum stress of the structure reveals that this is the case: the element with the largest von Mises stress achieves 95% of the yield stress of the material.

Figure 13 shows the resulting pressure distributions compared to the baseline aeroelastic analysis. Notice that the loading has changed substantially, particularly in the trailing edge region of the outboard portion of the wing. We believe this is a consequence of the fact that our structural box only extends to the 80% chord location and the loading in the trailing edge section is creating a rapid change in camber in that area.

Finally, Figure 14 shows a comparison of the geometries and the corresponding surface Mach number distributions of the baseline aero-structural analysis and the aero-structural optimized configuration. In this view the fuselage camber is obvious, but the changes in the wing shape and twist, as well as the aeroelastic deflections are difficult to notice. In fact, the tip deflections for this design case are on the order of 0.5% of the total span. The wing has thinned down considerably and is prevented from further decreases in thickness by the associated increase in structural weight that would result due to the stress constraints.

Conclusions

A methodology for coupled sensitivity analysis of high-fidelity aero-structural systems was presented. The sensitivities computed by the lagged-coupled adjoint method were compared to sensitivities given by the complex-step derivative approximation and shown to be extremely accurate, having an average relative error of 2%.

In realistic aero-structural design problems with

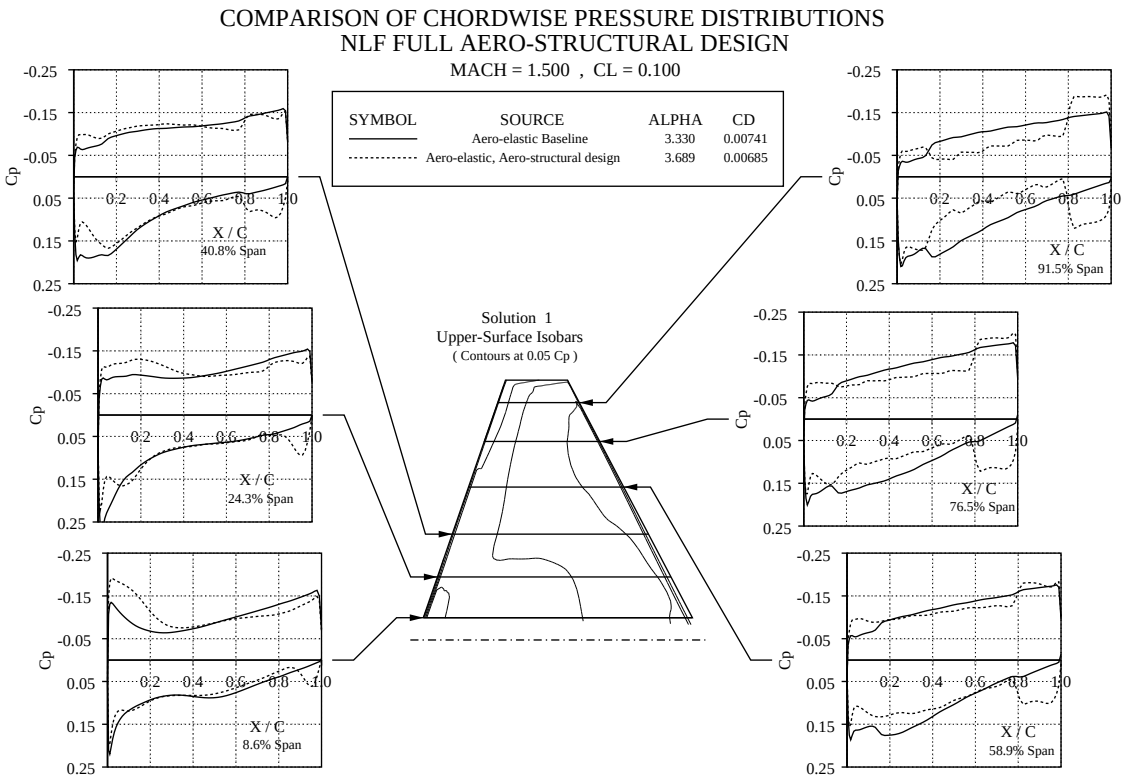

Fig. 13 Wing pressure distributions for aero-structural baseline and optimized designs, OML and structural design variables with K-S penalty function.

hundreds of design variables, there is a considerable reduction in computational cost when using the coupled-adjoint method as opposed to either finite-differences or the complex-step. This is due to the fact that the cost associated with the adjoint method is practically independent of the number of design variables.

Sensitivities computed using the presented methodology were successfully used to optimize the design of a supersonic business jet that was parameterized with a large number of aerodynamic and structural variables.

Future work in the development of our aero-structural design framework is expected to add further capability such that more realistic aircraft design problems can be solved. To achieve this we plan to add multiple flight conditions each one involving the calculation of a separate KS function coupled adjoint to enforce the various structural constraints. We also intend to add even more shape and wing planform design variables to the design cases as well as increase the geometric complexity of the configuration to include the presence of diverters and nacelles, as well as the empennage.

Acknowledgments

The first author acknowledges the support of the *Fundação para a Ciência e a Tecnologia* from the Portuguese government and the Stanford University Charles Lee Powell Fellowship. The second author has benefited greatly from the support of the AFOSR under Grant No. AF-F49620-01-1-0291 and the Raytheon Aircraft Preliminary Design Group. Finally we would like to thank the ASSET Research Corporation for providing the geometry and specifications for the natural laminar flow supersonic business jet.

References

[1]H. M. Adelman and R. T. Haftka. Sensitivity Analysis of Discrete Structural Systems. *AIAA Journal*, 24(5):823–832, May 1986.

[2]M. A. Akgün, R. T. Haftka, K. C. Wu, and J. L. Walsh. Sensitivity of Lumped Constraints Using the Adjoint Method. AIAA Paper 99-1314, Apr. 1999.

[3]K. G. Bhatia and J. Wertheimer. Aeroelastic Challenges for a High Speed Civil Transport. AIAA Paper 93-1478, Feb. 1993.

[4]S. A. Brown. Displacement Extrapolation for CFD+CSM Aeroelastic Analysis. AIAA Paper 97-1090, Jan. 1997.

[5]P. E. Gill, W. Murray, M. A. Saunders, and M. H. Wright. User's Guide for NPSOL (version 4.0). A FORTRAN Package Nonlinear Programming. *Technical Report SOL86-2*, Stanford University, Department of Operations Research, 1986.

[6]A. A. Giunta. A Novel Sensitivity Analysis Method for High Fidelity Multidisciplinary Optimization of Aero-Structural Systems. AIAA Paper 2000-0683, Jan. 2000.

[7]M. E. Holden. *Aeroelastic Optimization Using the Collo-*

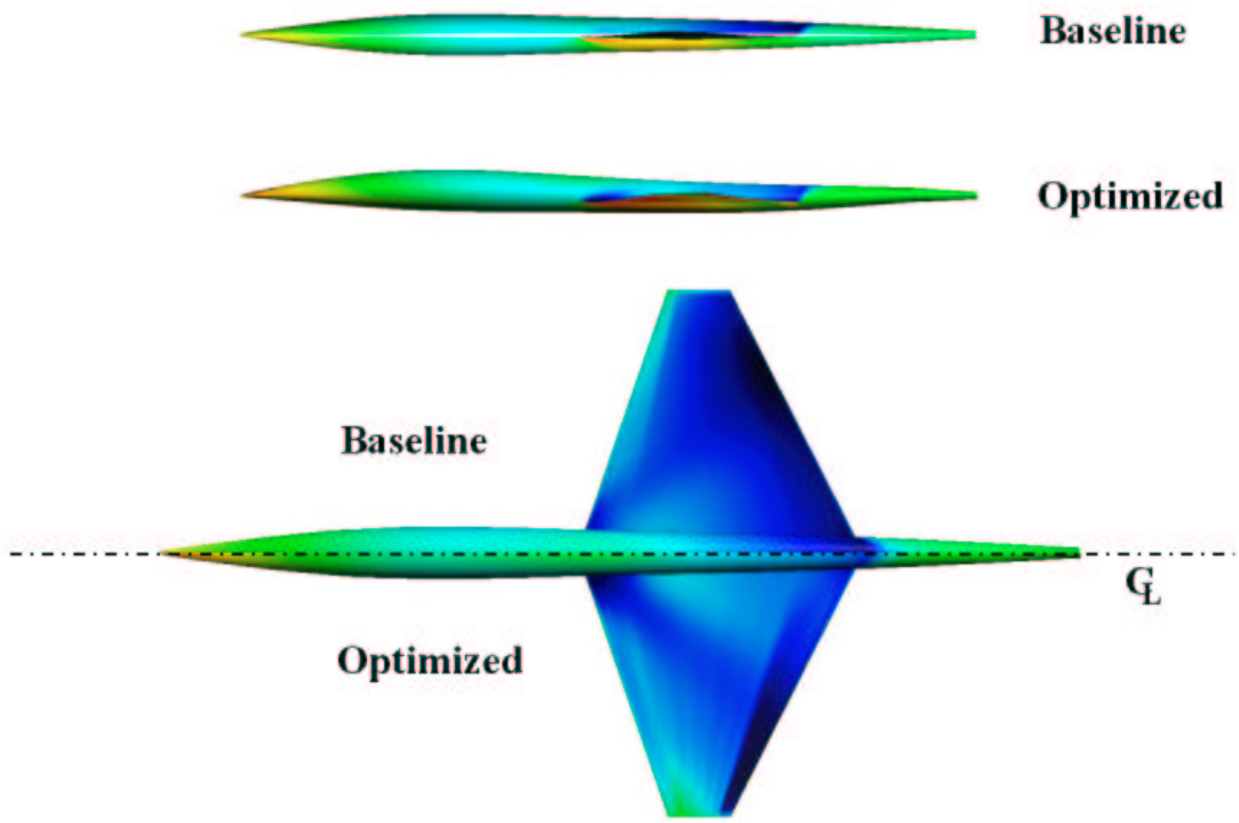

Fig. 14 Wing pressure distributions for aero-structural baseline and optimized designs.

cation Method. PhD thesis, Stanford University, Stanford, CA 94305, 1999.

[8]A. Jameson. Aerodynamic Design via Control Theory. *Journal of Scientific Computing*, 3:233–260, 1988.

[9]I. Kroo, R. Tracy, J. Chase, and P. Sturdza. Natural laminar flow for quiet and efficient supersonic aircraft. AIAA Paper 2002-0146, Jan. 2002.

[10]J. R. R. A. Martins, 2001. http://aero-comlab.stanford.edu/jmartins.

[11]J. R. R. A. Martins, J. J. Alonso, and J. Reuther. Aero-Structural Wing Design Optimization Using High-Fidelity Sensitivity Analysis. In *Proceedings — CEAS Conference on Multidisciplinary Aircraft Design Optimization, Cologne, Germany*, pages 211–226, June 2001.

[12]J. R. R. A. Martins, I. M. Kroo, and J. J. Alonso. An Automated Method for Sensitivity Analysis Using Complex Variables. AIAA Paper 2000-0689, Jan. 2000.

[13]J. R. R. A. Martins, P. Sturdza, and J. J. Alonso. The Connection Between the Complex-Step Derivative Approximation and Algorithmic Differentiation. AIAA Paper 2001-0921, Jan. 2001.

[14]K. Maute, M. Nikbay, and C. Farhat. Coupled Analytical Sensitivity Analysis and Optimization of Three-Dimensional Nonlinear Aeroelastic Systems. *AIAA Journal*, 39(11):2051–2061, Nov. 2001.

[15]J. Reuther, J. J. Alonso, M. R. A. Jameson, and D. Saunders. Constrained Multipoint Aerodynamic Shape Optimization Using an Adjoint Formulation and Parallel Computers: Part II. *Journal of Aircraft*, 36(1):61–74, 1999.

[16]J. Reuther, J. J. Alonso, A. Jameson, M. Rimlinger, and D. Saunders. Constrained Multipoint Aerodynamic Shape Optimization Using an Adjoint Formulation and Parallel Computers: Part I. *Journal of Aircraft*, 36(1):51–60, 1999.

[17]J. Reuther, J. J. Alonso, J. R. R. A. Martins, and S. C. Smith. A Coupled Aero-Structural Optimization Method for Complete Aircraft Configurations. AIAA Paper 99-0187, 1999.

[18]J. Reuther, J. J. Alonso, J. C. Vassberg, A. Jameson, and L. Martinelli. An Efficient Multiblock Method for Aerodynamic Analysis and Design on Distributed Memory Systems. AIAA Paper 97-1893, June 1997.

[19]J. Sobieszczanski-Sobieski. Sensitivity of Complex, Internally Coupled Systems. *AIAA Journal*, 28(1):153–160, Jan. 1990.

[20]J. Sobieszczanski-Sobieski and R. T. Haftka. Multidisciplinary Aerospace Design Optimization: Survey of Recent Developments. AIAA Paper 96-0711, Jan. 1996.

[21]S. R. Wakayama. *Lifting Surface Design using Multidisciplinary Optimization*. PhD thesis, Stanford University, Stanford, CA 94305, Dec. 1994.